International Research Journal on Advanced Engineering and Management
https://goldncloudpublications.com
https://doi.org/10.47392/IRJAEM.2025.076
e ISSN: 2584-2854
Volume: 03
Issue:03 March 2025
Page No: 514-519

Automated Blood Cell Detection and Counting

S Asha[1], R Swarna Lakshmi[2], P Dorathisha[3], M P Varshini[4]
[1]Assistant professor, Dept. of CSE, Sethu Institute of Tech., Virudhunagar, Tamil Nadu, India.
[2,3,4]UG Scholar, Dept. of CSE, Sethu Institute of Tech., Virudhunagar, Tamil Nadu, India.
Email ID: *sasha@sethu.ac.in[1], swarnaraj3011@gmail.com[2], dorathisha@gmail.com[3], varshiniprakash13@gmail.com[4]*

Abstract
In general, medical examinations, complete blood cell (CBC) counting has been essential. Common methods, such as automated analyzers and conventional manual counting, were greatly impacted by how medical professionals operated. Deep learning algorithms for computer-aided object detection have been successfully used in various visual applications in recent years. To precisely identify and count blood cells on blood smear images, we present in this research an architecture based on deep neural networks. A publicly available BCCD (Blood Cell Count and Detection) dataset assesses our architecture's performance. Images from blood smears are frequently low resolution, with overlapping and fuzzy blood cells. Preprocessing was done on the original photos, which included blurring, sharpening, enlargement, and picture augmentation. Five models are built here with various parameters in the suggested architecture. We thoroughly examine the variables influencing their performance and evaluate how well they identify red blood cells (RBC), white blood cells (WBC), and platelets. The outcomes of the experiment demonstrate that when blood cells do not excessively overlap, our algorithms are capable of reliably identifying blood cells.
Keywords: *convolutional neural network, deep learning, blood cell identification, and blood cell counting*

1. Introduction
Blood cells contain around 45% of blood tissue by volume, and an adult's blood contains generally five liters. Red blood cells (RBC), white blood cells (WBC), which include neutrophils, monocytes, eosinophils, lymphocytes, and basophils, and platelets are the three different types of blood cells. White blood cells help the immune system fight off illnesses, red blood cells are the primary means of transporting oxygen, and platelets have a coagulation function that helps heal wounds that have scabs. Clinically, blood composition is affected by both pathologic and physiological changes. As a result, blood testing is now a straightforward way to determine a person's health or identify illnesses. One of the traditional blood tests, complete blood cell (CBC) counting, detects and counts basic blood cells to analyze, monitor, and control blood variation [1]. But manual labor is laborious, time-consuming, and prone to error. Early in the 20th century, scientists started taking advantage of automated analyzers. Many studies use image processing methods and statistical or deep learning models to improve CBC counts on blood smear images as computing power increases but it is challenging to recognize blood cells since pictures are foggy and in low resolution. Numerous visual identification tasks have seen the successful application of convolutional neural networks (CNNs) [2]. CNNs are now a common method for handling medical image analysis because of their exceptional learning and feature extraction capabilities [3]. In this work, we provide a unique CNN-based deep learning architecture that enables accurate CBC counting while concurrently detecting and classifying blood cells on blood smear images. Here, five models with various configurations are built. Finally, we contrast and talk about the outcomes of the suggested models in various scenarios.

2. Materials and Methods
In order to locate and identify target cells in blood smear images, we provide a unique CNN-based deep learning architecture.

2.1 Proposed Architecture
Four steps of pre-processing are first applied to the blood smear images: blurring, sharpening,

International Research Journal on Advanced Engineering and Management
https://goldncloudpublications.com
https://doi.org/10.47392/IRJAEM.2025.076
e ISSN: 2584-2854
Volume: 03
Issue:03 March 2025
Page No: 514-519

enlargement, and picture augmentation. The core of the model was CNN, which was focused on extracting and creating basic feature maps. VGG-16[4] is used in this paper. In order to speculate on the locations of blood cells, we then included the Region Proposal Network (RPN) [. Potential feature vectors are created in the RoI (Region of Interest) Pooling layer by combining the data from the feature maps and RPN. Figure 1 shows The Proposed Architecture

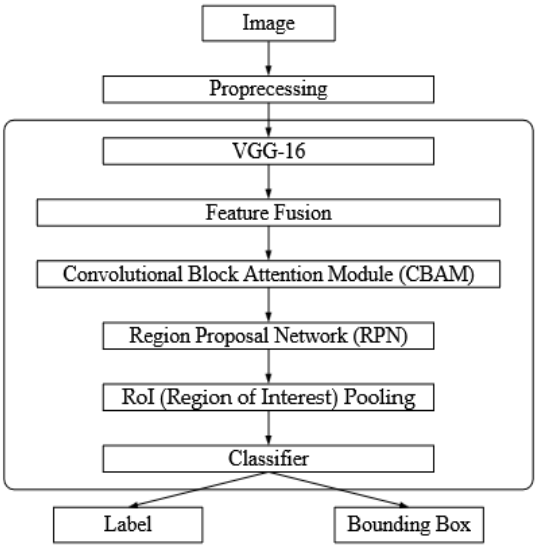

Figure 1 The Proposed Architecture

As seen in the upper portion of Figure 2, VGG-16 can be thought of as a composition of five blocks with a total of 13 convolutional layers, 5 pooling layers, and 3 fully-connected layers. VGG-16 uses 3 × 3 filters to produce feature maps with various resolutions. The pooling layer lowers the feature map resolution by max-pooling by a 2x2 window. The softmax layer, which is in charge of categorization, is the final completely connected layer. To highlight the important features, we also used the Convolutional Block Attention Module (CBAM) [5]. Given the input image, channel attention concentrates on what is significant. In addition to channel attention, spatial attention concentrates on where informative elements are located.The Faster R-CNN architecture was then used for blood cell counts, classification, and detection. Region Proposal Network (RPN) shares feature maps with CNN to provide region proposals. To create region proposals, or anchor boxes, and the matching lower-dimensional features, it moved a window across the feature map in the RPN layer.

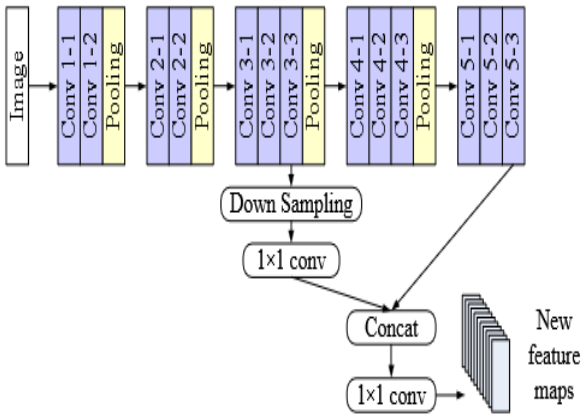

Figure 2 Feature Fusion in The Proposed Architecture

2.2 Evaluation Measures

For the evaluation of the bounding box and classifier, we employed three metrics: the confusion matrix, Distance-IoU (DIoU), and Intersection of Union (IoU). Equation (1) displays the IoU formula.

IoU = Ground Truth Bounding Box ∩ Predicted Bounding Box / Ground Truth Bounding Box ∪ Predicted Bounding Box (1)

Two overlapping boxes are shown to cross and unite in Figure 3. We assumed that the ground truth box was in Box B and the anticipated box was in Box A. The intersection is shown in red, and the union is shown in green. To figure out the IoU of Boxes A and B, the red area was divided by the green area. Figure 3 shows Intersection and Union of Two Overlapping Boxes A and B

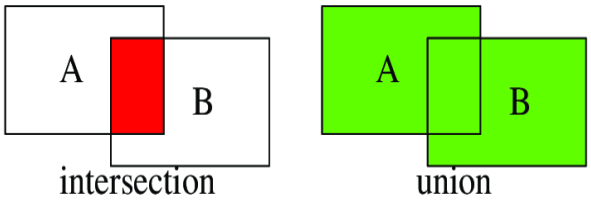

Figure 3 Intersection and Union of Two Overlapping Boxes A and B

International Research Journal on Advanced Engineering and Management
https://goldncloudpublications.com
https://doi.org/10.47392/IRJAEM.2025.076
e ISSN: 2584-2854
Volume: 03
Issue:03 March 2025
Page No: 514-519

Equation (2), as seen in Figure 4, computes DIoU by taking d, the Euclidean distance between the central points of the two overlapping boxes, and c, the diagonal length of the smallest rectangle that covers the two boxes.

DIoU = IoU − d2 / c2 **(2)**

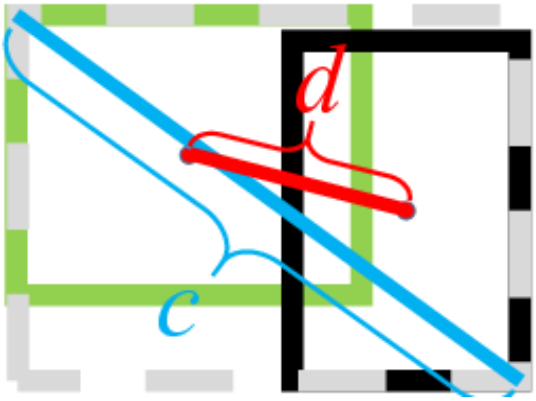

Figure 4 Distance-IoU (DIoU) Calculation of Two Overlapping Boxes

Equations (3) to (5) are used to determine the precision, recall, and F1 score.

Precision = TP / (TP+FP) **(3)**

Recall = TP / (TP+FN) **(4)**

F1 Score = 2 x Precision x Recall / Precision + Recall (5)

The following is what TP, FN, FP, and TN stand for in a binary classification:

When both the expected and actual classes are positive, it is known as true positive (TP).

When a positive sample is anticipated to be negative, it is known as false negative (FN).

When a negative sample is thought to be positive, it is known as false positive (FP).

When the actual and anticipated classes are both negative, it is known as true negative (TN).

3. Experiments and Results

3.1 Dataset Description

The Blood Cell Count and Detection (BCCD) dataset is used in the present study. It comes with 364 640 x 480-pixel blood smear images and an annotation file that offers more details about the picture. Figure in shows a blood smear image from the dataset, replete with bounding boxes and tagged blood cells. Figure 5 shows Original Image with Ground Truth Bounding Boxes and Labels

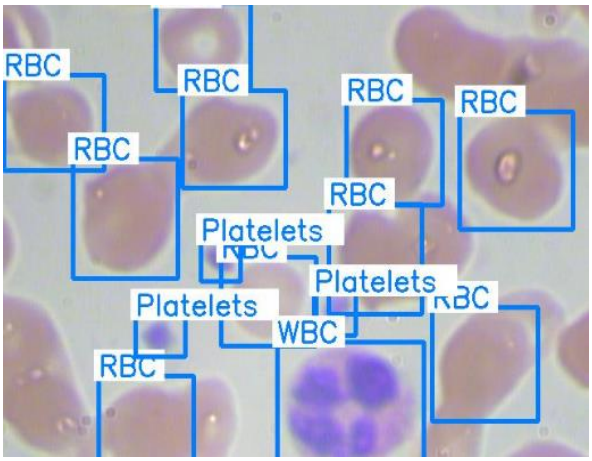

Figure 5 Original Image with Ground Truth Bounding Boxes and Labels

Two subsets of the dataset were randomly choosing: 20% of the images were for validation, whereas 80% of the images were for training. Table 1 BCCD Dataset

Table 1 BCCD Dataset

Blood Cells	Training (80%)	Validation (20%)
Red Blood Cell (RBC)	3310	843
White Blood Cell (WBC)	297	75
Platelets	301	60

4. Data Preprocessing

Four steps of pre-processing were first applied to the blood smear images: blurring, sharpening, enlargement, and picture augmentation. We changed the original photographs from RGB color space to grayscale in addition to applying rotation, flipping them horizontally and vertically to improve the quantity and variety of the images. We also employed

International Research Journal on Advanced Engineering and Management
https://goldncloudpublications.com
https://doi.org/10.47392/IRJAEM.2025.076
e ISSN: 2584-2854
Volume: 03
Issue:03 March 2025
Page No: 514-519

bicubic interpolation to expand the images because it is hard to discern small items like platelets. The fuzzy photos were then sharpened using the unsharp masking concept. There are three steps in the unsharp masking process: blur the original image, acquire the mask by subtracting the blurred image from the original, and then add a weighted piece of the mask back to the original. Equation (6) illustrates how we calculated an image's mask in this study by applying a 3 × 3 OpenCV built-in Laplacian filter and then subtracting a weighted portion of the mask from the image with a parameter k. fsharpen(x, y) = foriginal (x, y) − k × fmask(x, y) Next, in order to smooth out the photos, we blurred them using a 3 × 3 Gaussian is used in the present study. It comes with 364 640 x 480-pixel blood smear images and an annotation file kernel.

4.1 Model Setting

We built five models with various preprocessing configurations. While some used enhanced photos, others used bigger images. While some simply used RGB images, others used mixed grayscale and RGB images. Next, we established the RPN parameters in the five models for detecting blood cells in the dataset's images. Selecting the anchors' sizes and aspect ratios in RPN is essential for target-object detection. Three different blood cell types' pixel sizes are shown in Table 2. For RPN to detect objects, we choose 42, 86, and 170 pixels as anchor scales. Additionally, we use √2:1/√2, 1/√2:√2, and 1:1 as anchor aspect ratios. Consequently, RPN uses anchors of nine various diameters. The five suggested models' settings are listed in Table 3. Table 2 Blood Cell Information in Pixels.

Table 2 Blood Cell Information in Pixels

	Red Blood Cells			White Blood Cells			Platelets		
	Min	**Mean**	**Max**	**Min**	**Mean**	**Max**	**Min**	**Mean**	**Max**
x-axis	42	104	168	31	194	338	19	42	167
y-axis	39	100	166	27	174	286	23	40	135

Table 3 Model Settings

	Model 1	**Model 2**	**Model 3**	**Model 4**	**Model 5**
Input Size	480 × 640	600 × 800	720 × 960	480 × 640	480 × 640
Enlarge	No	Yes	Yes	No	No
Anchor Boxes Size	[42, 86, 170]	[53, 107, 213]	[64, 128, 256]	[42, 86, 170]	[42, 86, 170]
Sharpen	Yes	Yes	Yes	No	Yes
Images Color	Grayscale or RGB				RGB

4.2 Experiment Results

The experiment outcomes in the validation data of every model are displayed in Tables 4 and 5 with corresponding confidence scores of 0.9 and 0.8. More powerful than the rest are models 1, 2, and 3, which were trained using preprocessed photos in both RGB and grayscale color spaces. Model 1 is useful for the WBC recognition job. Model 3, which was trained using enlarged (1.5×) photos, gets a notable recall and F1score for RBC recognition tests. Model 5, which solely uses RGB pictures, has the highest precision but the lowest recall. Model 2, which was trained obtains the highest F1 scores for the platelet detection challenge. Table 4Results of The Validation Data of All Models When Confidence Score is 0.9.

International Research Journal on Advanced Engineering and Management
https://goldncloudpublications.com
https://doi.org/10.47392/IRJAEM.2025.076
e ISSN: 2584-2854
Volume: 03
Issue:03 March 2025
Page No: 514-519

Table 4 Results of The Validation Data of All Models When Confidence Score is 0.9

Type	Red Blood Cells			White Blood Cells			Platelets		
Index*	P	R	F1	P	R	F1	P	R	F1
Model 1	0.737	0.744	0.741	0.761	0.95	0.845	0.498	0.412	0.451
Model 2	0.794	0.673	0.729	0.521	0.614	0.564	0.529	0.492	0.51
Model 3	0.747	0.823	0.783	0.214	0.2	0.209	0.382	0.288	0.329
Model 4	0.731	0.762	0.747	0.704	0.886	0.784	0.381	0.431	0.405
Model 5	0.808	0.517	0.631	0.487	0.936	0.641	0.114	0.067	0.085

* P, R, and F1 refer to precision, recall, and F1-score, respectively.

Table 5 Results of The Validation Data of All Models When Confidence Score is 0.8

Type	Red Blood Cells			White Blood Cells			Platelets		
Index*	P	R	F1	P	R	F1	P	R	F1
Model 1	0.693	0.799	0.742	0.691	0.964	0.805	0.508	0.53	0.519
Model 2	0.761	0.748	0.755	0.536	0.7	0.607	0.47	0.67	0.553
Model 3	0.701	0.867	0.775	0.279	0.271	0.275	0.453	0.576	0.507
Model 4	0.684	0.814	0.743	0.662	0.921	0.77	0.351	0.518	0.418
Model 5	0.763	0.579	0.659	0.414	0.95	0.577	0.14	0.116	0.126

* P, R, and F1 refer to precision, recall, and F1-score, respectively.

Conclusions

We present a unique CNN-based architecture for blood cell counting and identification in this work. We use VGG-16 as the backbone of this design. Block attention mechanism (CBAM) and feature fusion enhance the feature maps produced by VGG-16. Blood cell detection makes use of Faster R-CNN's RPN and ROI Pooling techniques. Five versions with various configurations were built. Two confidence scores—0.9 and 0.8, respectively—were used for detection trials. Model 3, which employs images in both RGB and grayscale color spaces and enlarges input photos by 1.5 times, produced the best recalls for RBC detection, with 82.3% and 86.7% under two confidence values of 0.9 and 0.8, respectively. In the meantime, it obtained precision scores of 70.1% and 74.7% under the two confidence levels. Model 1, which employs both RBG and grayscale images and does image preprocessing, performs better than other models for WBC detection. Under a confidence score of 0.9, the precision and recall are 76.1% and 95%, respectively, whereas under a confidence score of 0.8, they are 69.1% and 96.4%, respectively. Compared to RBCs and WBCs, platelets are smaller and less numerous. Particularly when the platelets are grouped together, platelet detection is more difficult than RBC and WBC detection. It is apparent that, for unidentified reasons, not all blood cells have labels in the BCCD dataset's annotation files, which has a substantial effect on all models' accuracy.

Future Work

Some blood cells are visible near the image's edge in blood smear pictures. In order to accommodate defective blood cells, we are presently working on

International Research Journal on Advanced Engineering and Management
https://goldncloudpublications.com
https://doi.org/10.47392/IRJAEM.2025.076
e ISSN: 2584-2854
Volume: 03
Issue:03 March 2025
Page No: 514-519

enhancing our architecture using the idea presented in Mask R-CNN [50]. Recent approaches for object detection using deep learning are also being considered. In order to incorporate more blood cell samples for learning, we also search for more datasets of blood smear images. Data Availability Statement: The public dataset, Blood Cell Count and Detection (BCCD) dataset, used in the experiment is available at https://github.com/Shenggan/BCCD_Dataset.

Abbreviations

The following abbreviations are used in this manuscript:

ANN	Artificial Neural Network
CBAM	Convolutional Block Attention Module
CBC	Complete Blood Cell
CNN	Convolutional Neural Network
DIoU	Distance-IoU
HSV	Hue, Saturation, and Value
IoU	Intersection of Union
RBC	Red Blood Cell
RBG	Red, Blue, and Green
RoI	Region of Interest
RPN	Region Proposal Network
SVM	Support Vector Machine
WBC	White Blood Cell

References

[1]. Habibzadeh, M.; Krzy ˙zak, A.; Fevens, T. White Blood Cell Differential Counts Using Convolutional Neural Networks for Low Resolution Images. In Proceedings of the International Conference on Artificial Intelligence and Soft Computing, Zakopane, Poland, 9–13 June 2013; pp. 263–274.

[2]. Wang, W.; Yang, Y.; Wang, X.; Wang, W.; Li, J. Development of convolutional neural network and its application in image classification: A survey. Opt. Eng. 2019, 58, 040901. [CrossRef]

[3]. Premaladha, J.; Ravichandran, K.S. Novel approaches for diagnosing melanoma skin lesions through supervised and deep learning algorithms. J. Med. Syst. 2016, 40, 96. [CrossRef] [PubMed]

[4]. Simonyan, K.; Zisserman, A. Very deep convolutional networks for large-scale image recognition. In Proceedings of the 3rd International Conference on Learning Representations, San Diego, CA, USA, 7–9 May 2015.

[5]. Woo, S.; Park, J.; Lee, J.; Kweon, I.S. CBAM: Convolutional block attention module. In Proceedings of the European Conference on Computer Vision, Munich, Germany, 8–14 September 2018; pp. 3–19.

[6]. He, K.; Gkioxari, G.; Dollár, P.; Girshick, R.B. Mask R-CNN. In Proceedings of the IEEE International Conference on Computer Vision, Venice, Italy, 22–29 October 2017; pp. 2980–2988.